

Electroexcitation of giant multipole resonances in ^{40}Ca

著者	Torizuka Y., Itoh K., Shin Y. M., Kawazoe Y., Matsuzaki H., Takeda G.
journal or publication title	Physical Review. C
volume	11
number	4
page range	1174-1178
year	1975
URL	http://hdl.handle.net/10097/53378

doi: 10.1103/PhysRevC.11.1174

Electroexcitation of giant multipole resonances in ^{40}Ca

Y. Torizuka and K. Itoh

Laboratory of Nuclear Science, Tohoku University, Tomizawa, Sendai, Japan

Y. M. Shin

Accelerator Laboratory, University of Saskatchewan, Saskatoon, Canada

Y. Kawazoe, H. Matsuzaki, and G. Takeda

Department of Physics, Tohoku University, Sendai, Japan

(Received 17 December 1973; revised manuscript received 25 November 1974)

A study of inelastic electron scattering from ^{40}Ca in the momentum transfer range $q = 0.43\text{--}1.40\text{ fm}^{-1}$ has revealed strong excitations with quadrupole and octupole character which spread over the range of excitation energy $E_x = 10\text{--}25\text{ MeV}$. For comparison, a simple shell model calculation is made based on the quasielastic model.

$$\left[\text{NUCLEAR REACTIONS } ^{40}\text{Ca}(e, e'), \text{ measured } \sigma(E_e', \theta_e), E_x = 10\text{--}35\text{ MeV}, \right. \\ \left. q = 0.43\text{--}1.4\text{ fm}^{-1}. \text{ Enriched target.} \right]$$

I. INTRODUCTION

Systematic studies of inelastic scattering of electrons,¹⁻⁷ protons,⁸⁻¹¹ and other charged particles¹²⁻¹⁵ from medium and heavy nuclei have revealed the existence of a giant $E2$ -like resonance at the excitation energy $E_x \approx 65A^{-1/3}\text{ MeV}$ for almost all the nuclei investigated to date. A recent analysis of inelastic proton spectra in the continuum region in ^{40}Ca has shown that a large bump seen at 10–25 MeV is composed of dipole, quadrupole, and octupole states located at ~ 20 , ~ 17 , and $\sim 13.5\text{ MeV}$, respectively.⁸ A broad peak observed at $\sim 17\text{ MeV}$ in inelastic scattering of 71-MeV ^3He from ^{40}Ca has been ascribed as a giant quadrupole state.¹² Inelastic scattering of 115-MeV α particles from ^{40}Ca has also shown a prominent peak with quadrupole character at $\sim 18.25\text{ MeV}$ which exhausts 32% of the isoscalar energy-weighted sum rule (EWSR). Our previous investigation^{16,17} on the electroexcitation of ^{40}Ca indicated that the observed form factor was inconsistent with the excitation of the giant dipole resonance (GDR) alone and that considerable strength remains in the neighborhood of the diffraction minimum. A collective octupole excitation was then inferred at $\sim 19\text{ MeV}$ besides the GDR.¹⁷

The giant multipole resonance appears as a bump in the region of the nuclear continuum. Hence major uncertainties of giant resonance data arise from the separation of the resonant and nonresonant parts. In this paper we report the result of a reinvestigation of the excitation of giant multipole resonances of ^{40}Ca by inelastic scattering of electrons. The nuclear continuum is estimated

from a calculation based on a simple shell model, in order to understand the process.

II. EXPERIMENT

The experiment was performed with the Tohoku 300-MeV electron linear accelerator. The energy spectra of inelastically scattered electrons were measured at seven different values of the momentum transfer q ranging from 0.43 to 1.40 fm^{-1} . A 99.5% enriched ^{40}Ca target was employed and data were taken with an over-all energy resolution of 0.15%. The elastic cross section was also measured and used for the normalization of inelastic cross sections. Experimental details may be found elsewhere.¹⁸ In the present measurement the room background (target-out background) was equivalent to a cross section of $5 \times 10^{-35}\text{ cm}^2\text{ sr}^{-1}\text{ MeV}^{-1}$ and can be neglected. The so-called instrumental scattering (target-in background) was carefully investigated and found to be of the same order as the room background.

III. RESULT AND DISCUSSION

The measured energy spectra were corrected for the radiative effects by the method described earlier.¹⁸ In the present work, the tail subtraction has been improved by including the effect of the elastic form factor which was neglected previously. The resulting spectra are displayed in Fig. 1. One notes several peaks at the excitation energies of 10.3, 10.9, 11.8, 12.6, 13.8, 14.6, 16.9, and 19.5 MeV together with the large background of the nuclear continuum.

As in our previous analysis we have subtracted a smooth background from each spectrum and ob-

tained the resonant part. The background shape has been assumed to be $A(E_x - E_0)^{1/n}$, where E_x is the excitation energy of the nucleus, E_0 is the threshold energy ($= 7.04$ MeV) for α -particle emission, and A and n are parameters. A and n are restricted to the shape of the observed spectra in the region of high excitation energy ($E_x \geq 25$ MeV). If the q and E_x dependence of the GDR is known, then the values of A and n can be sought by fitting the observed spectra with the sum of the phenomenological form of the background and GDR at each q .

The GDR part of the observed cross section may be expressed in terms of the measured total photo-

absorption cross section¹⁹ $\sigma_\gamma(E_x)$ as follows:

$$d^2\sigma/d\Omega dE_x = (d\sigma/d\Omega)_{\text{Mott}} |F(q, E_x)|^2 \quad (1)$$

with

$$|F(q, E_x)|^2 = |f(q^2)|^2 (\Delta^4/q^4) E_x \sigma_\gamma(E_x), \quad (2)$$

where Δ is the four-momentum transfer. The form factor $|f(q^2)|^2$ is assumed to be given by the Tassie model²⁰ of GDR and was computed in the distorted wave Born approximation.²¹ With these assumptions, the parameters A and n have been determined, and the smooth background has been subtracted from the observed spectrum in order to obtain the resonant part of the cross section.

The resonance part of the cross section has been integrated from $E_x = 10$ to 25 MeV and divided by the Mott cross section. The result is plotted against the momentum transfer q (Fig. 2). Since it has been found that the observed q dependence cannot be reproduced with a single multipole excitation, the data have been fitted by mixing $E2$ and $E3$ components to the GDR as shown in Fig. 2. The $E2$ form factor has been calculated by the Tassie model, while that of the octupole excitation is assumed to be the same as that¹⁶ of the first 3^- state at 3.74 MeV in ^{40}Ca .

The decomposed form factors in Fig. 2 indicate that the total form factor at $q = 1.22 \text{ fm}^{-1}$ is dominated by $E3$ and the $(E1 + E2)$ component is minor ($\sim 10\%$). Accordingly, from the corresponding spectrum the spectral shape of the $E3$ excitation was obtained. The low q spectrum is mainly $E1 + E2$ ($\sim 95\%$ at $q = 0.43 \text{ fm}^{-1}$). The known GDR contribution was subtracted in order to obtain an

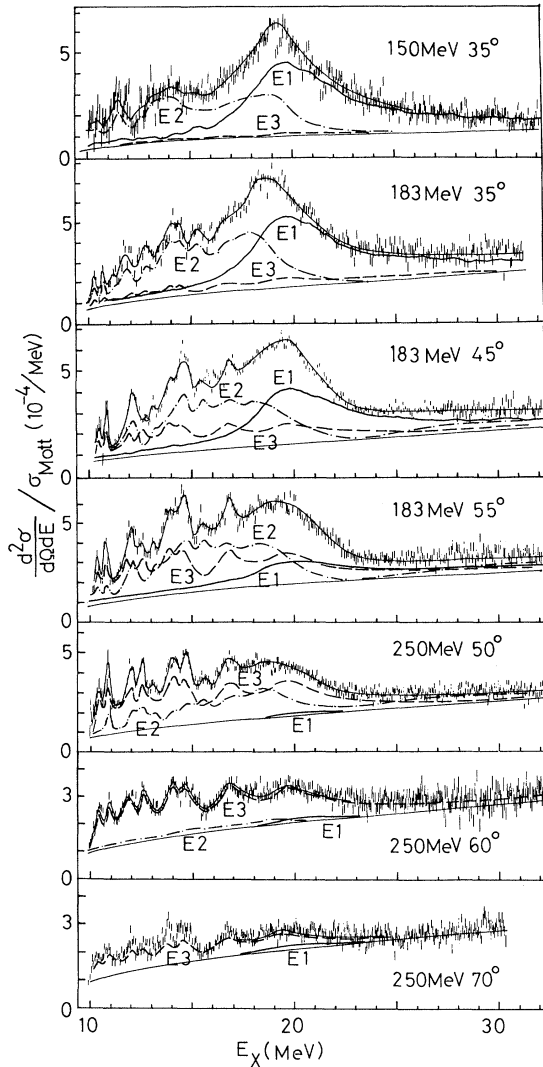


FIG. 1. The spectra of ^{40}Ca at various momentum transfers. The $E1$ (thick solid), $E2$ (dash-dotted) $E3$ (dashed), and the sum (thin solid) as well as the underlying background (smooth line) are shown.

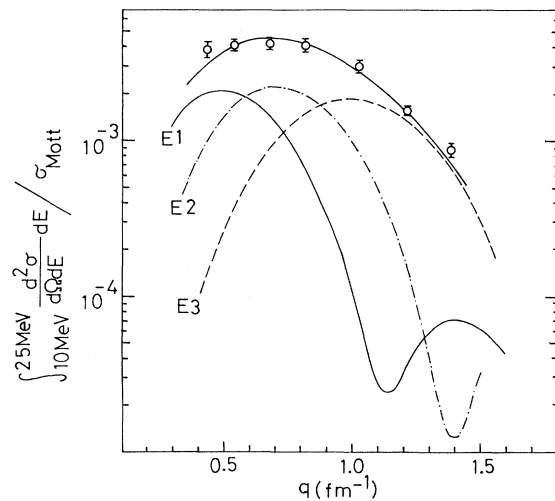


FIG. 2. The experimental form factor over the range 10–25 MeV. The solid, dash-dotted, dashed, and thick solid lines are the $E1$, $E2$, and $E3$ components and their sum, respectively.

TABLE I. Parameters for the background subtraction.

Energy (MeV)	Angle (deg)	n	$A (\times 10^{-4} \text{ MeV}^{-1})$
150	35	2	0.248
183	35	2	0.508
	45	2	0.447
	55	2	0.523
250	50	2	0.534
	60	2	0.531
	70	2	0.538

approximate shape of the $E2$ excitation. Using the q dependence of the form factors for the quadrupole and octupole excitations shown in Fig. 2, the parameters A and n , and the energy dependence of the quadrupole and octupole excitations have been varied to fit the observed spectra. The energy dependence of the quadrupole and octupole excitations which reproduce the observed spectra best are plotted in Fig. 1 with the values of A and n given in Table I.

The obtained quadrupole and octupole strengths are found to spread over the region of E_x between 10 and 25 MeV. Since the data have been taken at forward angles (35° – 70°), the multipole excitations are mainly due to the longitudinal (Coulomb) excitations of ^{40}Ca . From the q dependence of the longitudinal quadrupole ($C2$) and octupole ($C3$) excitations as described above, we can interpolate our data for the $C2$ and $C3$ excitations to the photon point ($q = E_x$) in the region of $E_x = 10 \sim 25$ MeV. This interpolation furnishes values of $B(E2, E_x)$ and $B(E3, E_x)$ which correspond to the strengths of the $E2$ and $E3$ photoabsorptions. These values are listed in Table II as a function of E_x for every 3 MeV interval in E_x . The errors, which are not larger than +15% and -30%, were estimated semi-empirically. The percentage of the corresponding classical energy weighted sum rule²² (isoscalar for $E2$ and $E3$) is also shown in the table. The total strength integrated over the whole energy region (10–25 MeV) becomes a large fraction of the sum rule limit for both $E2$ and $E3$ excitations, indicating strong collective nature of the observed quadrupole and octupole resonances.

The q dependence of the $C2$ strength is similar to that of the monopole in the Tassie model, and this similarity is also expected in more general classes of nuclear models. Therefore it is difficult to distinguish between the quadrupole ($C2$) and monopole ($C0$) excitation. However, various theoretical considerations^{23,24} place the centroid of the giant collective $E2$ resonance at about $E_x \simeq \sqrt{2} \hbar \omega \simeq \sqrt{2} \times 41 A^{-1/3} \text{ MeV} \simeq 17 \text{ MeV}$ for ^{40}Ca , at which our result shows the strongest excitation.

TABLE II. Values of $B(EL)$ and $|M(0)|^2$ and the percentage of the isoscalar energy-weighted sum rule (EWSR). The errors are +15% and -30%.

E_x (MeV)	L	$B(EL)$ ($e^2 \text{ fm}^{2L}$)	Percentage of EWSR ($T=0$)
10–13	2	72	8.2
	0	117	12.6
	3	2.97×10^3	6.3
13–16	2	144	20.6
	0	235	31.7
	3	2.93×10^3	7.9
16–19	2	148	25.6
	0	241	39.4
	3	2.71×10^3	8.8
19–22	2	57	11.6
	0	93	17.8
	3	2.43×10^3	9.2
22–25	2	0	0
	3	1.03×10^3	4.4
10–25	2	421	66
	0	688 ^a	102
	3	1.21×10^4	36.6

$$^a |M(0)|^2 = |\langle \sum_i \frac{1}{2} r_i^2 \rangle|^2 \text{ in fm}^4.$$

This leads us to believe the main contribution to our $C2$ -like resonance is most likely due to the quadrupole excitation rather than due to the monopole. However, the possibility of the existence of a significant fraction of the monopole strength cannot be excluded from our results alone. It is worthwhile to point out that if the $C2$ -like resonance is assumed to be due to a monopole excitation instead of $C2$, then the integrated monopole strength (from 10 to 25 MeV) amounts to 102% of the monopole sum rule limit.

In order to have some qualitative understanding of the background in continua and the importance of various multipole strengths, we have calculated the inelastically scattered electron spectra using a shell model, in which protons in a potential make transitions from a bound to a scattering state. No residual interactions have been taken into account. Such a model has been used in calculations of the quasielastic scattering process, and has been found to be quite successful in predicting the position and width of experimentally observed spectra²⁵ at large values of q and E_x .

We have employed in our calculations a Woods-Saxon type potential (a square well potential has also been used) used by Gibson and van Oostrum²⁶ with an imaginary part

$$-4iaW \frac{d}{dr} \{1 + \exp[(r-R)/a]\}^{-1}. \quad (3)$$

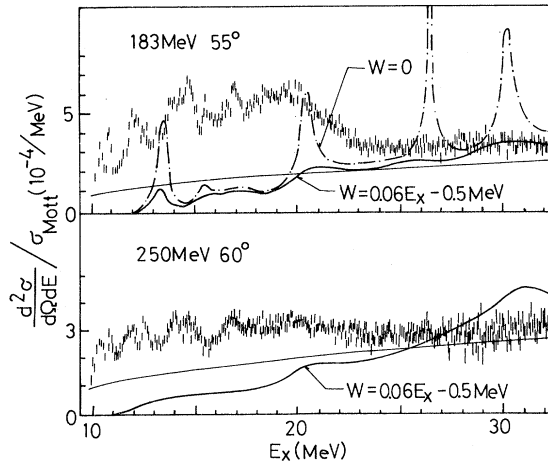


FIG. 3. The calculated excitation functions based on the quasielastic model. The phenomenological background curves are also shown.

If the imaginary potential is introduced, $W = (0.06E_x - 0.5)$ MeV has been used,²⁷ otherwise $W = 0$.

The calculated results show appreciable contributions from 2^λ -pole excitations up to $\lambda \approx qR = 4.28q$, as is expected, and the $C\lambda$ excitation shows peaks in the calculated spectrum at excitation energies corresponding to the resonance energies of the model as shown in Fig. 3.

The results have also predicted several discrete bound levels corresponding to the excitation of protons to the $f_{7/2}$ state which are not shown in the figure. However, when such levels were included in the sum, the resultant cross section became approximately the value of the observed cross section.

The width of the calculated peaks arises from the proton emission width and the imaginary potential. The latter represents the effect of a single proton-hole transition to more complex states, and its magnitude is difficult to estimate. We have used the value of W given in Ref. 27. Since the magnitude of W is small in comparison with the real part, the cross section for the formation of compound states is expected to be negligible and has not been taken into account in our calculation.

In order to extract the continuum background from the calculated result the following procedure has been taken: (1) we suppress those multipole strengths which would contribute to the giant multipole resonances if the residual interactions were to be effective, and (2) we introduce broadening of widths due to hole states, and average the strength using an appropriate weighting function of the width of each hole state (7 MeV for the

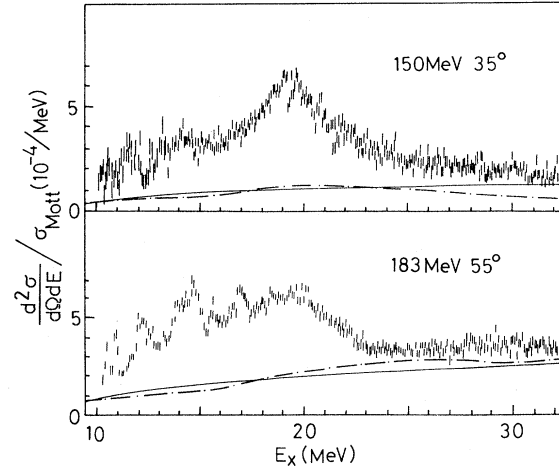


FIG. 4. The theoretical (dash-dot line) and phenomenological (full line) backgrounds.

$2s$ and $1d$ hole states and 20 MeV for the $1p$ and $1s$ hole states).²⁸

The hole width is assumed to be given by a Breit-Wigner type expression. All transitions except for the $T=1$ C1, $T=0$ C2, and $T=0$ C3 have been summed and smeared with the hole width, and the results are shown in Fig. 4. As is evident from the figure, a smooth spectrum which is consistent with the phenomenological background used in the data analysis is obtained. Figure 5 compares the integrated strengths of the phenomenological (open circles) and theoretical (full line) continuum backgrounds between 10 and 25 MeV. For comparison the integrated total (resonance plus background) cross section in the same range is shown. The comparison confirms the validity of the use of the phenomenological

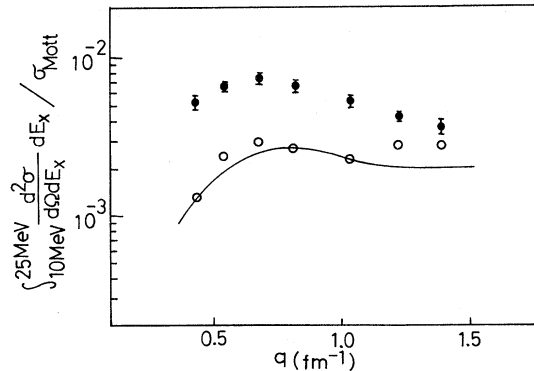


FIG. 5. The integrated values over 10–25 MeV for the cross section (closed circles), theoretical background (full line), and phenomenological background (open circles).

background. The background thus obtained here contains not only quasielastic scattering but also multipole resonances which are probably broad and fragmented.

In conclusion, our analysis on the electroexcitation of ^{40}Ca indicates the very strong collective nature of the quadrupole and octupole excitations in the range of excitation energy $E_x = 10 - 25$ MeV. The quadrupole strength is rather uniformly distributed over the range between 13 and 19 MeV while the octupole strength is distributed into the several narrow peaks at 10.3, 10.9, 11.8, 12.6, 13.8, 14.6, 16.9, and 19.5 MeV.

During the preparation of this paper the detailed random phase approximation theory²⁹⁻³¹ which calculates high multipole excitations in ^{40}Ca has been presented. The results are in good agreement with our experiment for both quadrupole and octupole strengths. The spectral shape in Fig. 1 is excellently reproduced by the theory³¹

with the sum of the several giant multipole resonances. Furthermore, this theory has divided the quadrupole component shown in Fig. 1 into the monopole resonance at ~ 14.0 MeV and quadrupole resonance at ~ 17.5 MeV. The inelastic α particle scattering^{15,32} which excites isoscalar 2^+ states strongly but 0^+ states weakly indicates a prominent peak (32% EWSR) at ~ 18.25 MeV and the strength is fragmented near 14 MeV. The $E2$ ($E0$) strength in Table II can be divided into the $E0$ (10 - 16 MeV) and $E2$ (16 - 22 MeV) excitations which exhaust the corresponding EWSR $\sim 44\%$ and $\sim 37\%$, respectively.

One of us (Y. M. S.) gratefully acknowledges the warm hospitality of the Tohoku University during his stay. The numerical calculation has been performed at the Computer Center of Tohoku University.

-
- ¹R. Pitthan and Th. Walcher, Phys. Lett. **36B**, 563 (1971).
- ²F. R. Buskirk, H.-D. Gräf, R. Pitthan, H. Theissen, O. Titze, and Th. Walcher, Phys. Lett. **42B**, 194 (1972).
- ³S. Fukuda and Y. Torizuka, Phys. Rev. Lett. **29**, 1109 (1972).
- ⁴M. Nagao and Y. Torizuka, Phys. Rev. Lett. **30**, 1068 (1973).
- ⁵S. Klawansky, H. W. Kendall, A. K. Kerman, and D. Isabelle, Phys. Rev. C **7**, 795 (1972).
- ⁶Y. Torizuka *et al.*, in *Proceedings of the International Conference on Nuclear Structure Studies Using Electron Scattering and Photoreactions, Sendai, Japan, 1972*, edited by K. Shoda and H. Ui (Tohoku Univ., Sendai, Japan, 1972), p. 171.
- ⁷Y. Torizuka *et al.*, in *Proceedings of the International Conference on Photoneuclear Reactions and Applications, Asilomar, 1973*, edited by B. L. Berman (Lawrence Livermore Laboratory, Univ. of California, 1973), Vol. 1, p. 675.
- ⁸M. B. Lewis, Phys. Rev. Lett. **29**, 1257 (1972).
- ⁹M. B. Lewis and F. E. Bertrand, Nucl. Phys. **A196**, 337 (1972).
- ¹⁰G. R. Satchler, Nucl. Phys. **A195**, 1 (1972).
- ¹¹M. B. Lewis, F. E. Bertrand, and D. J. Horen, Phys. Rev. C **8**, 398 (1973).
- ¹²A. Moalem, W. Benenson, and G. M. Crawley, Phys. Rev. Lett. **31**, 482 (1973).
- ¹³M. B. Lewis, Phys. Rev. C **7**, 2041 (1973).
- ¹⁴M. B. Lewis, in *Proceedings of the International Conference on Photoneuclear Reactions and Applications, Asilomar, California, 1973* (see Ref. 7), p. 685.
- ¹⁵L. L. Rutledge, Jr., and J. C. Hiebert, Phys. Rev. Lett. **32**, 551 (1974).
- ¹⁶K. Itoh, M. Oyamada, and Y. Torizuka, Phys. Rev. C **2**, 2181 (1970).
- ¹⁷K. Itoh, T. Saito, and Y. Torizuka, in *Proceedings of the International Conference on Nuclear Structure Studies Using Electron Scattering and Photoreactions, Sendai, Japan, 1972* (see Ref. 6), p. 14.
- ¹⁸A. Yamaguchi, T. Terasawa, K. Nakahara, and Y. Torizuka, Phys. Rev. C **3**, 1750 (1971).
- ¹⁹J. Ahrens, H. Borchert, H. B. Eppler, H. Gimm, H. Gundrum, P. Riehn, G. Sita Ram, A. Zieger, M. Kröning, and B. Ziegler, in *Proceedings of the International Conference on Nuclear Structure Studies Using Electron Scattering and Photoreactions, Sendai, Japan, 1972* (see Ref. 6), p. 213.
- ²⁰L. J. Tassie, Aust. J. Phys. **9**, 407 (1956).
- ²¹S. T. Tuan, L. E. Wright, and D. S. Onley, Nucl. Instrum. Methods **60**, 70 (1968).
- ²²For example, A. M. Lane, *Nuclear Theory* (Benjamin, New York, 1965).
- ²³I. Hamamoto, in *Proceedings of the International Conference on Nuclear Structure Studies Using Electron Scattering and Photoreactions, Sendai, Japan, 1972* (see Ref. 6), p. 205.
- ²⁴T. Suzuki, Nucl. Phys. **A217**, 182 (1973).
- ²⁵T. W. Donnelly, Nucl. Phys. **A150**, 393 (1970).
- ²⁶B. F. Gibson and K. J. van Oostrum, Nucl. Phys. **A90**, 159 (1967).
- ²⁷M. Marangoni and A. M. Saruis, Nucl. Phys. **A132**, 649 (1969).
- ²⁸K. Nakamura, S. Hiramatsu, T. Kamae, H. Muramatsu, N. Izutsu, and Y. Watase, Phys. Rev. Lett. **33**, 853 (1974).
- ²⁹G. Bertsch and S. F. Tsai, unpublished.
- ³⁰S. Krewald and J. Speth, Phys. Lett. **52B**, 295 (1974).
- ³¹G. R. Hammerstein, H. McManus, A. Moalem, and T. T. S. Kuo, Phys. Lett. **49B**, 235 (1974).
- ³²J. M. Moss, C. M. Rozsa, J. D. Bronson, and D. H. Youngblood, report, Cyclotron Institute, Texas A.&M. University (unpublished).